Biointerface Research in Applied Chemistry
Open-Access Journal (ISSN: 2069-5837)

Article
Volume 13, Issue 3, 2023, 243
https://doi.org/10.33263/BRIAC133.243

LP-SBA-15/Ketorolac Nanocomposite: Development, Characterization, and Mathematical Modeling of Controlled Keto Release

Jorgelina Cussa [1], Juliana M. Juarez [1], Marcos B. Gomez Costa [1], Oscar A. Anunziata [1,*]

[1] Center for Research in Nanoscience and Nanotechnology (NANOTEC), Córdoba Regional Faculty, National Technological University, Córdoba, Argentina
* Correspondence: oanunziata@frc.utn.edu.ar (O.A.A.);

Scopus Author ID 7003541531
Received: 6.12.2022; Accepted: 28.12.2022; Published: 7.06.2022

Abstract: Drug-controlled release systems can keep the level of drugs in precise doses in the body above the optimal level and with low toxicity. We propose the nanomaterial LP-SBA-15 as an attractive new host for drug delivery systems due to its high biocompatibility, in vivo biodegradability, and low toxicity. LP-SBA-15/Ketorolac was prepared and characterized by XRD, FTIR, UV-Vis DRS, TEM, and texture analysis, determining the adsorption capacity and its release and achieving the required therapeutic efficacy. The host shows the ordered mesoporous nanochannels with a diameter of 11-12 nm, maintaining the structure with the incorporation of Keto. The mechanism of drug release from the LP-SBA-15 host was evaluated. Different mathematical models were used to adjust the experimental data, the Ritger-Peppas model followed by the Weibull model the best ones. The promising results we obtained for the release of the drug thoroughly using the new material, reaching a rapid initial release rate, and maintaining a constant rate afterward, allow us to maintain the concentration of the drug in the therapeutic efficacy range, applying it largely to the treatment of diseases that require a rapid response.

Keywords: LP-SBA-15; ketorolac tromethamine; nanostructured host; drug-delivering device; nanoscale medicine.

1. Introduction

Mesostructured materials represent a new generation of porous solids characterized by regular pores in the nanometer size range (2-50 nm) and susceptible to manipulation depending on the needs of each application through different synthesis procedures. The characteristics include significant surface development, defined pore structure, and high capacity for the adsorption of organic substrates, allowing the considerable potential for different applications. The concept of nanotechnology encompasses those fields of technology in which materials, substances, and devices of small dimensions, smaller than the micron, namely, on a nanometric scale, are studied, obtained, and manipulated thoroughly. The field of Nanotechnology includes, in addition to the areas of knowledge related to its origin, other fields in its more remote beginnings but for which it has great importance, such as Biology, Medicine, or the Environment. Since the first reports of mesoporous materials from C. Kresge [1], new fields of exploration have been opened in intra-crystal inclusion chemistry [2], generating materials with optimized mechanical, physical, and chemical properties, which can be intelligently controlled in a range. Therefore, they are an attractive option to achieve a comprehensive and well-defined

system that completes the detailed study of fundamental properties, which has a direct application in different technological problems [3,4], such as Nano bioengineering applications as in "modified drugs release [5]. Controlled drug release technology is gaining relevance in the emerging pharmaceutical and drug industries [6-8]. Nanotechnology allows the release of the drug to be minimally invasive as it enables the manufacture of devices on a nanometer scale. This size permits these devices to pass through pores and cell membranes. Another major advantage is that the drug's effectiveness is increased through the precise control of the required dose and size, morphology, and surface properties of the composite [9], preventing enzymatic or acidic decomposition of susceptible drugs in the gastrointestinal region [10]. The delivery of drugs is an expanding area that primarily focuses on the search for drugs [11]. The controlled drug delivery points can provide accurate delivery when and where therapeutic drug agents are at the destination, keeping the concentration of the drug directly in the organism at the optimal time and below the tolerance level, improving the effectiveness of the treatment and reducing the risk of damage [12]. Nanotechnology applied to the administration, diagnosis, and development of drugs represents a change in medicine of this century. This field will generate important results; hence, the drug is monitored for each day or week according to the condition to be addressed. Nanoreservoirs for drug delivery can be inorganic or organic nanostructures and comply with biocompatibility and non-toxicity. In this way, less non-desirable influences and higher drug intake are expected [13]. The focus has been mainly on nanoscience and nanotechnology in the recent past.

The application of nanoscience and nanotechnology in medicine, and more specifically in the field of drug delivery, is set to increase rapidly. Recent progress in developing new materials has increased research interest in sample preparation due to their desirable characteristics and benefits compared to traditional and commercial drugs. Nanoparticle drug delivery systems present an exciting opportunity as alternative platforms to improve the efficacy and safety of currently used drugs. For this reason, the use of new materials is extensively explored in the manufacture of nanomedicine [14,15]. Mesoporous materials have unique pore size, higher surface area, and pore volume and have been widely employed as carriers for controlled drug delivery. Compared with amorphous colloidal and porous silica, mesoporous silicas exhibit higher loading of drugs and provide a controlled drug release if modified by functionalization [16]. Larger pore sizes are attainable by mixing additives with greater critical molecular size, as well as by modifying the reaction conditions [17, 18]. The incorporation of drugs in hosts of the SBA (Santa Barbara Silicates) family improves the bioavailability of poorly water-soluble drug molecules due to their large surface area and Si-OH-type interaction sites, ordered pore systems of 5-10 nm, allowing higher host loadings and homogeneous and reproducible drug release [19]. The organic surface modification of this large-pore mesoporous silica has raised considerable interest in different research fields such as catalysis, adsorption, separation processes, and drug delivery systems [20].

SBA-15 is mesoporous material with a large, controlled pore size and highly ordered hexagonal topology [5]. The pore size of SBA-15 is usually 6 nm in diameter [21]. Numerous reports concerning the application of SBA-15 as a host in the drug delivery system report promising results [5,22-24]. Mesoporous silica LP-SBA-15 (large pore) material is a crystalline mesoporous molecular framework with an ordered and precise mesoporous system [25]. This material has the attractive properties of the uniform pore size of 12 nm running along the same direction; moreover, due to high biocompatibility, in vivo biodegradability, and low toxicity

[26,27], thus mesostructured silica with a large pore (LP-SBA-15) is a new promising host for drug delivery systems.

Ketorolac tromethamine is a nonsteroidal anti-inflammatory drug with potent analgesic and moderate anti-inflammatory activity. It is widely used in clinics intra-muscularly or intravenously to treat moderate to moderately severe pain in perioperative, postoperative, and emergency department settings [28]. This significant dissociation between analgesic and anti-inflammatory effects provided the foundation for advancing medicine as an exceptional anti-inflammatory and analgesic [29-32]. Concerning nonsteroidal anti-inflammatory drugs NSAIDs, numerous reports relating to the application of formulations based on composite KETO/nanomaterial have been published [32,33]. Recently, we reported a promising drug storage material for the effective encapsulation and controlled release of KETO; the study demonstrated the storage capacity and release properties of SBA-15 containing KETO. The release of KETO contained in SBA-15 can offer a significant improvement in controlled drug release and enhance a good analgesic effect [5]. Advancing in this sense, this work studies the usage of mesoporous LP-SBA-15 with large pore size, which by the effect of the interaction between the host and drug molecules and by diffusion through the porosity of LP-SBA-15, leads to a substantial contribution to controlled drug release. Academic and industrial researchers have highlighted nanomaterial-based drug delivery.

As the first report found in the literature on this specific composite, the main objective of this research is to evaluate the adsorption performance and storage qualities of LP-SBA-15 / KETO and the release, achieving the required therapeutic efficacy.

2. Materials and Methods

2.1. Materials.

Tetraethylorthosilicate (TEOS, 98%, Sigma–Aldrich), Poly(ethylene glycol)-block-poly(propylene glycol)-block-poly (ethylene glycol), ($EO_{20}PO_{70}EO_{20}$, P123-Sigma–Aldrich, ≥99.0%, FLUKA), Ammonium fluoride (NH_4F, ≥99.0%, Sigma-Aldrich), 1,3,5-Triisopropylbenzene ($C_6H_3[(CH(CH_3)_2]_3$, 95%, Sigma-Aldrich) Ketorolac Tromethamine (99.5%, Fluka; KETO), Buffer pH 7 (Ciccarelli) and HCl (Ciccarelli, 36-38 % wt.).

2.2. Characterization.

Structural and textural characteristics, imaging, and vibrational studies were conducted employing the following equipment: X'Pert Pro PANalytical, ASAP 2020, JEOL 2100F, and JASCO 5300 FTIR, respectively. UV-Vis studies were made in Jasco 7800 equipment. Ultraviolet-visible diffuse reflectance spectroscopy (UV-Vis DRS) was used to determine the presence of the drug inside the host, recorded with a Perkin Elmer Lamba 650 spectrophotometer equipped with a diffuse reflectance accessory.

2.3. Synthesis of LP-SBA-15.

To synthesize mesoporous SBA-15 material with pore sizes greater than that of a traditional SBA-15, we followed a method that uses an expanding agent of micelles [34]. Specifically, 2.4 g of the template ingredient (Pluronic 123 copolymer, Aldrich) and 0.027 g of NH_4F dissolved in 85 mL HCl (1.3 M) at ambient temperature were placed in a water bath at 17ºC for 1h. Later, 5.5 mL of tetraethylorthosilicate (TEOS, Aldrich) and 1.2 mL of 1,3,5-

triisopropyl benzene (TIPB, Aldrich) were incorporated. Later, 5.5 mL of tetraethylorthosilicate (TEOS, Aldrich) and 1.2 mL of 1,3,5-triisopropyl benzene (TIPB, Aldrich) were incorporated and maintained with mechanical agitation at this temperature for 24h. The remaining white suspensions were then aged at 100°C (LP) under static and autogenic pressure 24 h. The solid products were collected by filtration. To eliminate the templating agent, the solid obtained was heated under a flow of N2 at 20 mL/min at 470°C and then heated again at 550 °C under static air for 6 h. The resultant mesoporous material large pore SBA-15 was named LP-SBA-15.

2.4. Drug-loading procedure.

The drug (ketorolac tromethamine) was dissolved in 20 mL of ethanol with dynamic agitation at 37°C (35 mg/mL), and then 15 mg/mL of the mesoporous silica material was introduced. The mixture was maintained at ambient temperature for 24 h in constant stirring in a sealed reactor to avoid any evaporation of ethanol. Subsequently, the mixture was filtered and dry for 24 h at 37 °C. The samples were designated LP-SBA-15 / KETO.

2.5. Drug release studies.

The release of the drug was evaluated by reproducing the physiological conditions and immersing the composite in an HCl solution (0.1 M) for the first two hours and in Buffer solution pH = 7 for the following hours to reproduce the conditions of the organism. The entire test was conducted at 37 °C with constant stirring. Release experiments were conducted to evaluate the requisite efficacy of the treatment. At varying times, 5 mL samples were taken and filtered. The study was performed by UV-Vis spectrophotometry to evaluate the quantity of KETO released at λ = 346 nm.

Furthermore, a reference solution of HCl (0.1 M) and Buffer pH = 7, with diverse concentrations of KETO, was set to produce the curve of absorbance versus concentration. Since in the study of *in vitro* release, it is necessary to achieve the system carefully, to work with safety, precision, and quality of the drug delivery systems based on nanoparticles, the variety of available methods makes it difficult to compare the results obtained. Thus, as reported by Weng et al. [35], a sample and separately (SS) method combining USP II (United States Pharmacopoeia USP) with centrifugal ultrafiltration (CU) was used to achieve efficient separation of the free drug from the reservoir containing it.

The models used to adjust the Ketorolac release mechanism from the LP-SBA-15 matrix are the first-order kinetic model, the Higuchi model, the Schott model, the Weibull model, and the Ritger and Peppas model. These mathematical models are the most widely used to determine the drug release mechanism of a delivery system. This method has been applied to the absorption and disposal of several drugs [36]. It can be implemented to describe the dissolution of water-soluble drugs contained in some porous structures, although it is difficult to conceptualize this mechanism theoretically.

$$\frac{M_t}{M_\infty} = 1 - e^{-kt} \quad (1)$$

where Mt / M∞ is the fraction of drug released at time t and k is the first-order release constant.

This relationship can be applied to explain the dissolution of the drug from some form of pharmaceutical administration, like those with water-soluble drugs in porous arrays [37], in which the host releases the drug in proportion to the amount of drug left inside so that the quantity of drug liberated per unit of time diminishes.

Higuchi [38,39] developed several theoretical models to study the release of water-soluble and poorly soluble drugs incorporated into semisolid and solid matrices. This model describes drug release as a diffusion process based on Fick's law, dependent on the square root of the release time. It is possible to simplify the Higuchi model as

$$\frac{M_t}{M_\infty} = k\sqrt{t} \quad (2)$$

Where k is the Higuchi dissolution constant, this relationship can also be applied to describe the dissolution of drugs through various types of modified-release pharmaceutical delivery modes, such as some transdermal systems and tablet matrices of water-soluble drugs [40,41].

The Schott model [42] develops second-order release kinetics:

$$\frac{dM_t}{dt} = k(M_\infty - M_t)^2 \quad (3)$$

The solution integrating between the limits M = 0 when t = 0 and Mt results in [42]:

$$M_t = \frac{kM_\infty^2 t}{1+kM_\infty t} \quad (4)$$

For the weight fraction of drug released, the following would remain

$$\frac{M_t}{M_\infty} = \frac{kM_\infty t}{1+kM_\infty t} \quad (5)$$

where k is the second-order velocity constant according to the Schott model.

The Weibull function (or exponential stretching function) was proposed to depict the performance of a considerable number of conditions for an unknown analytical form [43].

Although the Weibull function provides reasonable fits has no physical basis since it is not derived from the diffusion equation. Therefore, the Weibull fit is not necessarily associated with the physical variables that describe the process (like diffusivity), the geometry of the system, or the structure of the host matrix. In particular, the Weibull feature can be seen, at best, as an empirical engagement function that provides an acceptable global fit with no determination of the correct boundaries [44]. A generalized experiential equation outlined by Weibull was adjusted to the process of delivery [45]. It is commonly used in controlled drug release studies [46,47]. The Weibull equation, applied to the release or dissolution of the drug from dosage procedures, indicates the cumulative fraction of drug release in the Mt / M∞ solution at time t, per

$$\frac{M_t}{M_\infty} = 1 - e^{\frac{(t-T)^b}{a}} \quad (6)$$

From this equation, the scaling factor, a, determines the time scale of the process. The parameter T means the delay time (latency phase) until the start of the release process, and in certain instances, it would be zero. The parameter of form b defines the curve as exponential.

Korsmeyer and Peppas [48] and Ritger and Peppas [49,50] designed a simple, semi-empirical method that exponentially relates the release of the drug to time t. These works presented their equation analyzing the drug release in a polymer matrix with behavior according to Fick's law (Fickian behavior) and with a deviation from said law (non-Fickian behavior). The equation that describes the model is the following:

$$\frac{M_t}{M_\infty} = \mathrm{k}t^n \quad (7)$$

where k is the constant proportional to the release rate that incorporates both structural and geometric features of the way the drug is administered, and n is the exponent of release, which indicates the release mechanism of the drug.

3. Results and Discussion

3.1. X-ray diffraction and textural properties.

To determine the structure of the host and the composite (LP-SBA-15 and LP-SBA-15 / KETO), X-ray diffraction analyses were performed (Figures 1 and 2). The low angle XRD pattern (Figure 1) for the host LP-SBA-15 displays a high reflection peak (1 0 0) and two minor peaks (second-and third-order peaks), corresponding to the diffraction planes (1 1 0) and (2 0 0)). These peaks can be indexed with a hexagonal crystallographic structure of the P6mm group [51]. For the LP-SBA-15 / KETO composite, the diffraction pattern shows a small enlargement of the reflection peak, as well as a move toward a greater 2Θ. This performance can be ascribed to a slight alteration of the mesoporous channels due to integrating the drug within the host channels.

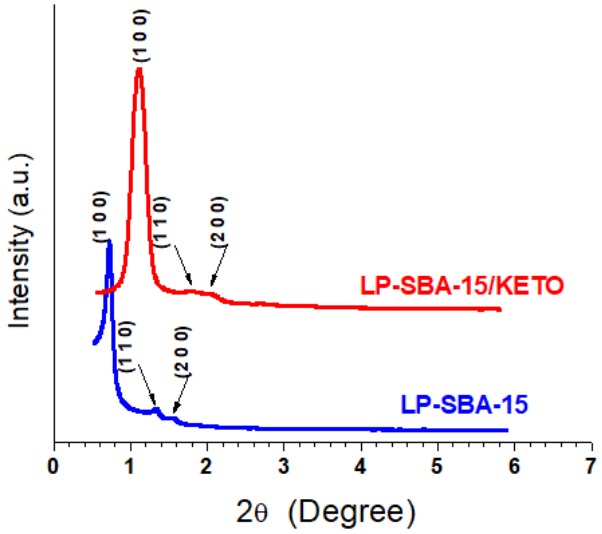

Figure 1. X-ray diffraction pattern of LP-SBA-15 and LP-SBA-15 / KETO composite.

The high-angle X-ray diffraction pattern allows for determining the drug within the LP-SBA-15 mesoporous material. In Figure 2, we can see that the LP-SBA-15 host exhibits an amorphous behavior, while the pure drug has typical peaks because of the crystalline structure [52].

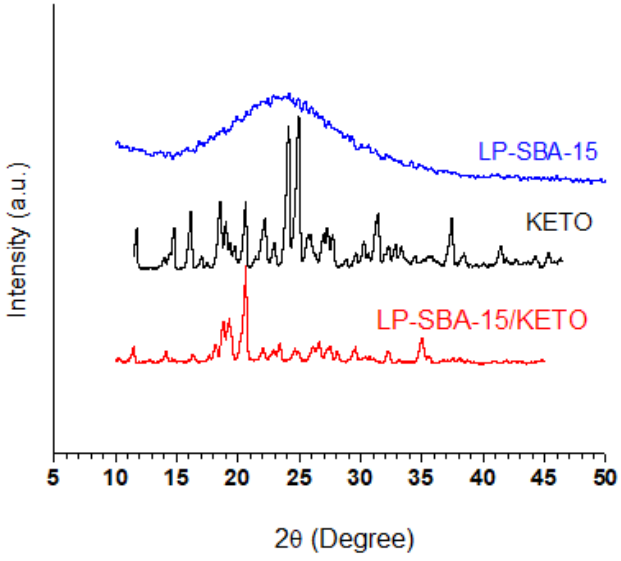

Figure 2. X-ray diffraction pattern of LP-SBA-15 and LP-SBA-15 / KETO composite.

Alternatively, the LP-SBA-15 / KETO composite shows some typical KETO peaks, suggesting that the drug incorporated in the host stays in a crystalline state. The KETO embedded in the channels of the LP-SBA-15 is probably ordered differently or has a phase shift.

Table 1. Textural Properties of the samples.

Sample	Area BET m^2/g	Vol. of mesopore V_P (cm^3 g^{-1})	Pore diameter (nm)
LP-SBA-15	436	1.1	12
LP-SBA-15/KETO	250	0.8	7.5

Table 1 summarizes the textural properties of the LP-SBA-15 host and the LP-SBA-15 / KETO composite, including surface area (BET), pore-volume, and pore diameter. While the composite area is significantly smaller than that of the host, it maintained its characteristic structure after loading the drug within the host, in agreement with the XRD studies. As can be seen, there is also a significant reduction in the pore diameter of the LP-SBA-15/KETO, which would indicate that we find the drug in the host's pores. There is a reduction of the surface area due to the blockage of the host's channels with its consequent reduction of pores.

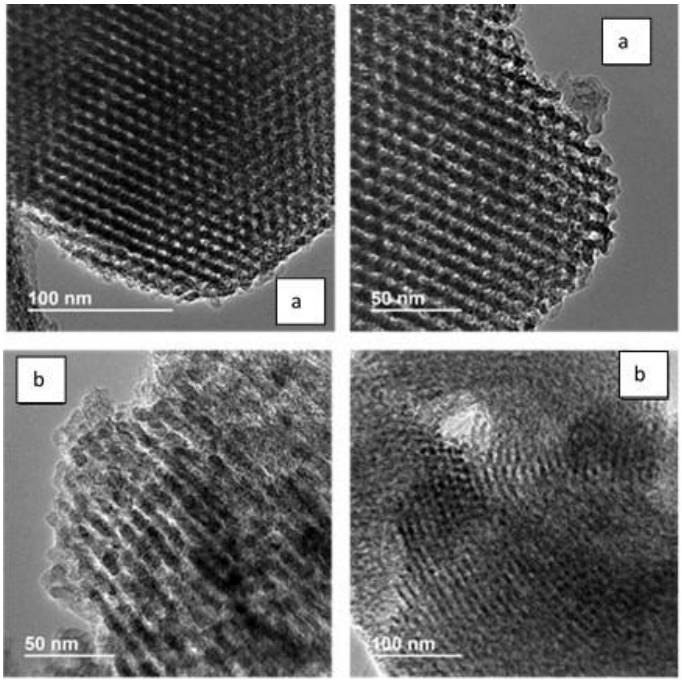

Figure 3. TEM images of a) LP-SBA-15 and b) LP-SBA-15/KETO.

Figure 3 shows the TEM images of both nanomaterials. The host shows an array of ordered mesoporous nanochannels with 11-12 nm diameter. Additionally, the sample with the adsorbed drug maintains the ordered mesostructure of the host, in agreement with the different analyses performed.

3.2. FTIR studies.

Figure 4 shows FTIR spectra for the pure drug KETO, the host LP-SBA-15, and the composite LP-SBA-15/KETO. The host presents characteristic bands of ordered silicate nanomaterial. A large proportion of silanol groups in the siliceous material LP-SBA-15 can be observed, giving rise to two hydroxyl stretch bands, broadband at 3458 cm^{-1} due to isolated terminal silanol groups (Si-OH) hydrogen-bonding silanol groups. It also presents a signal at 969 cm^{-1}, assigned to asymmetric stretching of Si-O bond neighboring surface silanol groups.

For the host, the bands at around 1085 cm^{-1} (Si-O asymmetric stretching) and 800 cm^{-1} (Si-O symmetric stretching) are due to the intrinsic vibration of SiO_4 tetrahedral [53]. For the pure drug, the band at 3357 cm^{-1} corresponds to N-H and O-H stretching vibrations. Two bands at 3100 and 725 cm^{-1} suggest aromatic C–H stretching and aromatic C-H bending vibrations, respectively. The band at 1385 cm^{-1} can be assigned to an aliphatic C–H bending vibration; at 1600 cm^{-1}, we observe a band representing a carboxylic acid C=O stretching vibration. Another two bands are present in the spectra; the band at 1566 cm^{-1} is ascribed to carbonyl C=O stretching vibration, and a band at 895 cm^{-1} shows the monosubstituted phenyl ring. In the region between 1454-1450 cm^{-1} C=C ring, we can observe antisymmetric elongation [52,54]. The composited obtained LP-SBA-15/KETO presents characteristics of both drug bands and vibrations of the inorganic framework. This behavior shows that the drug was absorbed into the host channel and doesn't affect the surface and the chemical structure or composition of KETO.

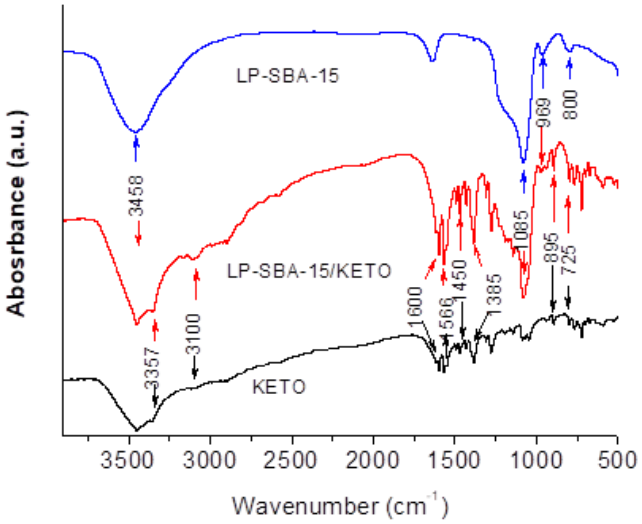

Figure 4. FTIR of LP-SBA-15, KETO, and LP-SBA-15 / KETO.

3.3. Ultraviolet-visible diffuse reflectance spectroscopy.

Figure 5 shows the UV-Vis DRS spectrum of Ketorolac-Thrometamine included in LP-SBA-15 nanochannels.

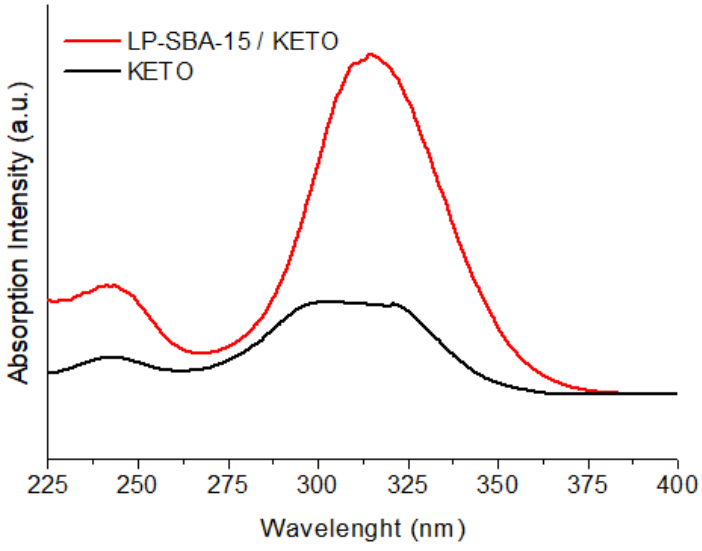

Figure 5. The ultraviolet-visible diffuse reflectance spectrum of KETO/LP-SBA-15 and pure KETO.

The characteristic bands of KETO can be observed approximately at 240 and 315 nm [55]. The aluminosilicate does not adsorb at these wavenumbers. The band at 240 nm is associated with π- π∗ electronic transitions involved in the aromatic group of the drug [56]. This would indicate that KETO does not significantly change its structure when adsorbed on the host ' 'channel's surface (LP-SBA-15).

3.4. Ketorolac- tromethamine adsorption and release studies.

Mathematical modeling, otherwise called the law of power, has been widely employed to depict the administration of drugs from various controlled-release dosage forms of pharmaceuticals or administration [57-59]. The drug release mechanism from the LP-SBA-15 matrix was assessed by fitting the data to the theoretical models described above. For this purpose, the least-squares and the Levenberg-Marquardt method were used to minimize the objective function. We show the results in Figure 6.

Table 2 shows the fitting coefficients and the statistics values for each model for the Ritger-Peppas and Weibull models. We analyzed four statistics to select the best model, the coefficient of determination (R2), the adjusted R^2, SEE (sum of squared errors), and S, the standard deviation of the distance between the data values and the fitted values. The two functions fit similarly, and it is difficult to select one, but according to the statistics presented, the best fit would be the Ritger-Peppas model by little. All statistics values indicate that the best model is the Ritger-Peppas model. And considering that our system release drug from the nanometric channels framework, where diffusion processes could be dominant, we select the Ritger-Peppas model where its equation would allow us to analyze the drug release from the nanoporous framework. Therefore, the other models (First-Order, Higuchi, and Schott) do not accurately describe the drug delivery data achieved in our study.

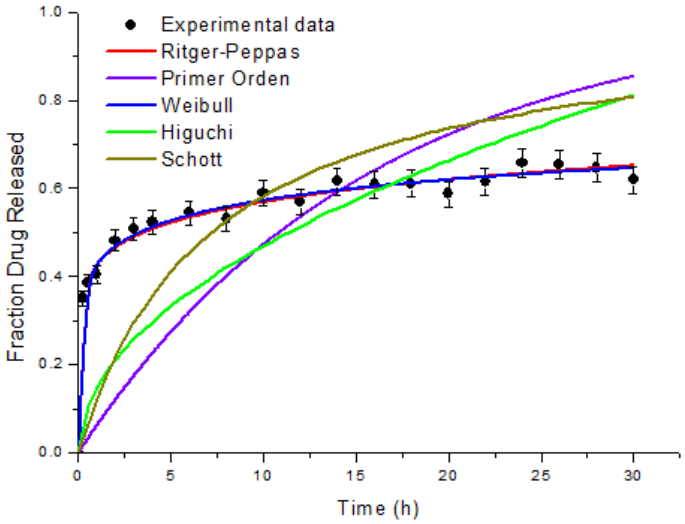

Figure 6. Fitting of experimental data using the first-order mathematical models, Higuchi, Schott, Weibull, and Ritger-Peppas.

Table 2. Coefficients of fit and statistics.

Mathematical model	Adjustment parameters	R^2	R_{adj}^2	SEE	S
Weibull	T= 0.00 a=1.80 b=0.19	0.97	0.96	0.0062	0.019
Ritger-Peppas	k=0.43 n=0.12	0.98	0.98	0.0056	0.018

R^2 coefficient of determination, R_{adj}^2 adjusted R^2, SEE sum of squared errors, and S standard deviation of the distance between the data values and the fitted values

In Figure 7, we can see the release of Ketorolac-Tromethamine from the porous matrix of LP-SBA-15 over time in the two release media, presenting two controls, one of administration from tablets (Dolten) and the other of direct dissolution of the drug. According to Figure 7, a rapid release was observed initially, and then the medium continued to release more slowly. As the Weibull model is experiential, it is not based on kinetics. It has certain shortcomings and has undergone considerable critical examination. [43, 60-62], for example, there is no kinetic support and only defines, although not adequately described, the kinetic dissolution properties of the drug, and it is not a single factor associated and related to the inherent dissolution rate of the drug. In the Ritger-Peppas model, when the exponent is equal to 0.5, it corresponds to the Higuchi equation. The release occurs through the Fick diffusion mechanism (Fickian diffusion), controlled diffusion, or Type I. Values above 0.5 are related to abnormal diffusion mechanisms (non-Fickian diffusion). In particular, when n = 1, we refer to zero-order kinetics, what Peppas calls a non-Fickian diffusion limit case, naming it "Type II" [50]. The values of n> 1 appear when the release time is high; it is an anomalous non-Fickian diffusion mechanism or "Supertype II". Finally, the values of n <0.5 are assigned to the existence of pores in the polymer array and consequent diffusion through the array and the pores full of dissolution media [63,64]. This situation is called the mechanism of behavior below the Fickian. This mechanism could remain Fickian [65], so the model fits better with the experimental data. The result of n presented in Table 2 is <0.5 since it includes the drug in a series of mesoporous materials of the LP-SBA-15 matrix, showing that the release mechanism could deviate from the Fick trend [66].

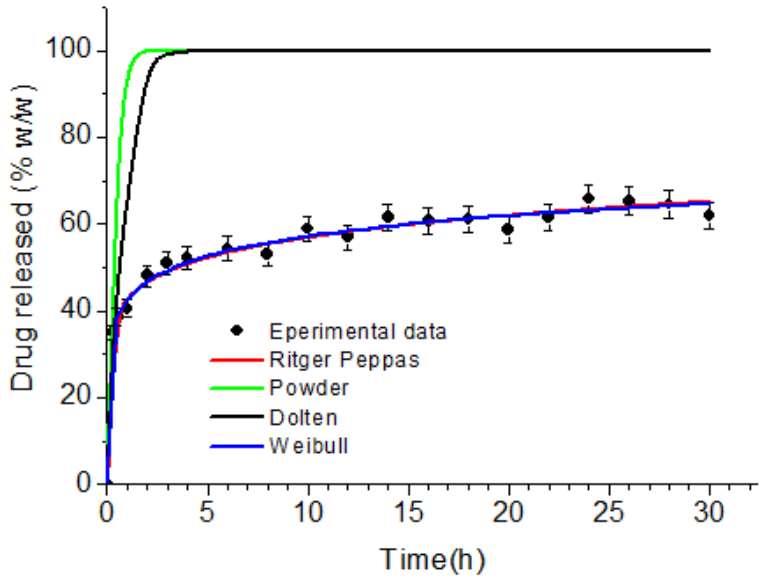

Figure 7. Release of Ketorolac contained in LP-SBA-15 with the adjustment of Ritger-Peppas and Weibull and controls.

For the mesoporous material LP-SBA-15, n = 0.12 indicates transport trends that deviate from ' 'Fick's law, as previously suggested by Rokhade et al. [67]. The 0.5 deviations may be because the host is a porous matrix of nanometric channels, which causes a divergence of the laws of diffusion. Because of the porous structure of the LP-SBA-15, as proven by microscopic examinations, this assumption can be considered [68-70].

The initial release is rapid and can be attributed to the reason that Ketorolac molecules are placed on the external surface of the silica or in the outlet of the mesopores. Nevertheless, a slower liberation of the bulkier remaining drug is observed after rapid initial release. The surface morphology and the LP-SBA-15 matrix allow a gradual release at high times. Surface

chemical groups (such as Si-OH groups) [71], surface-anchoring sites, and the position of the oxygenated units in the pore network of nanostructured silicates affect their adsorption performance if they are employed such as adsorbents in aqueous solutions. Note that the bonds formed across the drug molecules and material and by diffusion through the porosity of the host influenced the release rate.

4. Conclusions

This work shows a promising drug storage material for effective encapsulation and controlled release of KETO, achieving the required therapeutic efficacy. Studies show that KETO was adsorbed on the channel surface of LP-SBA-15 without affecting the structure or chemical composition of KETO. Controlled drug delivery systems can achieve precise delivery at the time and place of destination, keeping the concentration of the drug at points in the body within the optimal range and below the toxicity threshold. The study also demonstrates the storage capacity and release properties of LP-SBA-15 containing KETO. The models used to adjust the release mechanism of the Ketorolac from the LP-SBA-15 matrix are the first-order kinetic model, the Higuchi model, the Schott model, the Weibull model, and the Ritger and Peppas model being the last two ones that best adjust the experimental data. Many authors, among which we include ourselves, have studied the reduction of the fluctuations of the drug level in the blood, the reduction in the dose and frequency of administration, possible improvement in the selectivity of the pharmacological activity, and a prolonged therapeutic effect. However, among the biggest challenges is the loss of flexibility to adjust the dose, the risk of releasing a high dose of the drug immediately because of a system failure, and the risk of accumulation, items on which this work provides important advances. The release of KETO contained in LP-SBA-15 can significantly improve the controlled release of the drug and the analgesic and anti-inflammatory effects, positively influenced by the links formed between the host and drug molecules and by diffusion through the host porosity.

Funding

This research was funded by CONICET-Argentine, grant number 11220200100771CO, 2021-2023.

Acknowledgments

JC, JJ, MGC and OAA, CONICET researchers, NANOTEC-UTN-FRC.

Conflicts of Interest

The authors declare no conflict of interest.

References

1. Kresge, C.; Leonowicz, M.; Roth, W.; Vartuli, J. and Beck, J. Ordered mesoporous molecular sieves synthesized by a liquid-crystal template mechanism. *Nature* **1992**, *359*, 710-712, https://doi.org/10.1038/359710a0.
2. De Risi, C.; Bortolini, O.; Brandolese, A.; Di Carmine, G.; Ragno, D.; Massi, A. Recent Advances in Continuous-Flow Organocatalysis for Process Intensification. *React. Chem. Eng.* **2020**, *5*, 1017–1052, https://doi.org/10.1039/d0re00076k.

3. El Sayeh, F.; Abou, E.E.; Hassan, M.; El-Maraghy, D. Ketorolac tromethamine floating beads for oral application: Characterization and in vitro/in vivo evaluation. *Saudi Pharm. J.* **2014**, *22*, 349-359, https://doi.org/10.1016/j.jsps.2013.06.006.
4. Zhu, S.; Chen, C.; Chen, Z.; Liu, X.; Li, Y.; Shi, Y.; Zhang, D. Thermo-responsive polymer-functionalized mesoporous carbon for controlled drug release. *Mater. Chem. Phys.* **2011**, *126*, 357–363, https://doi.org/10.1016/j.matchemphys.2010.11.013.
5. Cussa, J.; Juárez, J.; Gómez Costa, M.; Anunziata O. Nanostructured SBA-15 host applied in ketorolac tromethamine release system. *J. Mater. Sci. Mater. Med.* **2017**, *28*, https://doi.org/10.1007/s10856-017-5925-4.
6. Adepu, S.; Ramakrishna, S. Controlled Drug Delivery Systems: Current Status and Future Directions. *Molecules* **2021**, *26*, https://doi.org/10.3390/molecules26195905.
7. Leonetti, B.; Perin, A.; Ambrosi E.; Sponchia, G.; Sgarbossa, P.; Castellin, A.; Riello, P; Scarso, A. Mesoporous zirconia nanoparticles as drug delivery systems: Drug loading, stability and release. *J. Drug Deliv. Sci. and Technol.* **2021**, *61*, https://doi.org/10.1016/j.jddst.2020.102189.
8. Anselmo, A.; Gokarn, Y.; Mitragotri, S. Non-invasive delivery strategies for biologics. *Nat. Rev. Drug Discov.* **2019**, *18*, 19–40, https://doi.org/10.1038/nrd.2018.183.
9. Uhrich, K.; Cannizzaro, S.; Langer, R.; Shakesheff, K. Polymeric systems for controlled drug release. *Chem. Rev.* **1999**, *99*, 3181-3198, https://doi.org/10.1021/cr940351u.
10. Qiu, X.; Leporatti, S.; Donath, E.; Möhwald, H. Studies on the Drug Release Properties of Polysaccharide Multilayers Encapsulated Ibuprofen Microparticles. *Langmuir* **2001**, *17*, 5375-5380, https://doi.org/10.1021/la010201w.
11. Tran; P.; Zhang, L.; Webster, T. Carbon nanofibers and carbon nanotubes in regenerative medicine. *Adv. Drug Deliv. Rev.* **2009**, *61*, 1097–1114, https://doi.org/10.1016/j.addr.2009.07.010.
12. Wang, S. Ordered mesoporous materials for drug delivery. *Microp. and Mesop. Mat.* **2009**, *117*, 1-9, https://doi.org/10.1016/j.micromeso.2008.07.002.
13. Bawa, R. Nanodrug delivery: avoiding the patents minefield and ensuring commercial viability Patents and nanomedicine. *Nanomed. NBM* **2007**, *2-3*, 351–374, https://doi.org/10.1016/j.nano.2007.10.038.
14. Sierra, I.; Morante-Zarcero, S. New Advances in Food Sample Preparation With Nanomaterials for Organic Contaminants Analysis by Liquid Chromatography. *Nanomater. Chromatography* **2018**, *5*, 118–154, https://doi.org/10.1016/B978-0-12-812792-6.00005-4.
15. González, L.; Morante-Zarcero, S.; Pérez-Quintanilla, D.; Sierra, I. Hydroxymethylfurfural determination in cereal and insect bars by high-performance liquid chromatography-mass spectrometry employing a functionalized mesostructured silica as sorbent in solid-phase extraction. *J. Chromatography A* **2020**, *1622*, https://doi.org/10.1016/j.chroma.2020.461124.
16. Wang, S. Ordered mesoporous materials for drug delivery. *Microp. and Mesop. Mat.* **2009**, *117*, 1–9, https://doi.org/10.1016/j.micromeso.2008.07.002.
17. Gonzalez-Delgado, I.; Segura, Y.; Martín, A.; Lopez-Muñoz, M.J.; Morales, G. b-galactosidase covalent immobilization over large-pore mesoporous silica supports for the production of high galacto-oligosaccharides (GOS). *Microp. and Mesop. Mat.* **2018**, *257*, 51–61, https://doi.org/10.1016/J.MICROMESO.2017.08.020.
18. Awoke, Y.; Chebude, Y.; Díaz, I. Controlling Particle Morphology and Pore Size in the Synthesis of Ordered Mesoporous Materials. *Molecules* **2020**, *25*, https://doi.org/10.3390/molecules25214909.
19. Farjadian, F.; Roointan, A.; Mohammadi-Samani, S.; Hosseini, M. Mesoporous silica nanoparticles: synthesis, pharmaceutical applications, biodistribution, and biosafety assessment. *Chem. Eng. J.* **2019**, *359*, 684-705, https://doi.org/10.1016/j.cej.2018.11.156.
20. Yu, Y.; Wang, Z.; Wang, R.; Jin, J.; Zhu, Y. Short-Term Oral Administration of Mesoporous Silica Nanoparticles Potentially Induced Colon Inflammation in Rats Through Alteration of Gut Microbiota. *Int. J. Nanomed.* **2021**,*16*, 881–893, http://doi.org/10.2147/IJN.S295575.
21. Speil, N.; Hoffmann, F.; Brieler, F.J.; Fröba, M. From the outside to the inside: Elucidation of the mechanism of pseudomorphic transformation of SBA-15 into MCM-41 by following its time-resolved conversion . *Microp. Mesop. Mat.* **2021**, *328*, https://doi.org/10.1016/j.micromeso.2021.111442.
22. Mehmood, Y.; Khan, I.U.; Shahzad, Y.; Khan, R.U.; Iqbal, M.S.; Khan, H.A.; Khalid, I.; Yousaf, A.M.; Khalid, S.H.; Asghar, S.; Asif, M.; Hussain, T.; Shah, S.U. In-vitro and in-vivo evaluation of velpatasvir-loaded mesoporous silica scaffolds. A prospective carrier for drug bioavailability enhancement. *Pharmaceutics* **2020**, *12*, https://doi.org/10.3390/pharmaceutics12040307.
23. Yang, G.; Li, Z.; Wu, F.; Chen, M.; Wang, R.; Zhu, H.; Li, Q.; Yuan, Y. Improving solubility and bioavailability of breviscapine with mesoporous silica nanoparticles prepared using ultrasound-assisted solution-enhanced dispersion by supercritical fluids method. *Int. J. of Nanomed.* **2020**, *15*, 1661-1675, https://doi.org/10.2147/IJN.S238337.
24. Song, S.W.; Hidajat, K.; Kawi, S. Functionalized SBA-15 Materials as Carriers for Controlled Drug Delivery: Influence of Surface Properties on Matrix−Drug Interactions. *Langmuir* **2005**, *21*, 9568–9575, https://doi.org/10.1021/la051167e.

25. III,. Li, Y.; Huang, X.; Hai, G.; Lv, J.; Tao, Z.; Wang, G. Crystallization of C18 in mesoporous silica: Effect of surface functionalization and nanoconfinement. *Chem. Eng. J.* **2021**, *428*, https://doi.org/10.1016/j.cej.2021.131075.
26. Wang, Z.; Sun, R.; Wang, P.; Wang, W. Unit-cell wide SBA-15 type mesoporous silica nanoparticles. *Microp. Mesop. Mat.* **2021**, *328*, https://doi.org/10.1016/j.micromeso.2021.111491.
27. Cao, L.; Man, T.; Kruk, M.; Synthesis of Ultra-Large-Pore SBA-15 Silica with Two-Dimensional Hexagonal Structure Using Triisopropylbenzene As Micelle Expander. *Chem. Mater.* **2009**, *21*, 1144–1153, https://doi.org/10.1021/cm8012733.
28. Li, C.; Li, C.; Liu, Z.; Li, Q.; Yan, X.; Liu, Y.; Lu, W. Enhancement in bioavailability of ketorolac tromethamine via intranasal in situ hydrogel based on poloxamer. *Int. J. Pharm.* **2014**, *474*, 123–133, https://doi.org/10.1016/j.ijpharm.2014.08.023.
29. Cloesmeijer, M.; van Esdonk, M.; Lynn A.; Smits A.; Tibboel, D.; Daali, Y.; Olkkola, K.; Allegaert, K.; Mian, P. Impact of enantiomer-specific changes in pharmacokinetics between infants and adults on the target concentration of racemic Ketorolac: A pooled analysis. *Br. J. Clin. Pharmacol.* **2021**, *87*, 1443-1454, https://doi.org/10.1111/bcp.14547.
30. Benoit, D.; Overby, C.; Sims, K.; Ackun-Farmmer, M. Drug delivery systems. In: *Biomaterials Science (Fourth Edition) An Introduction to Materials in Medicine.* Academic Press, **2020**; pp. 1237–1266, https://doi.org/10.1016/B978-0-12-816137-1.00078-7.
31. Jain, K. An overview of drug delivery systems. *Drug Deliv. Syst.* **2020**, *2059*, 1–54, https://doi.org/10.1007/978-1-4939-9798-5_1.
32. Naz F.; Siddique Y.; Targets N. Nanotechnology: Its application in treating neurodegenerative diseases. CNS Neurol. Disord. *Drug Targets* **2021**, *20*, 34–53, https://doi.org/10.2174/1871527319666200916121515.
33. Morsi, N.; Ghorab, D.; Refai, H.; Teba, H. Ketorolac tromethamine loaded nanodispersion incorporated into thermosensitive in situ gel for prolonged ocular delivery. *Int. J. Pharm.* **2016,** *506*, 57–67, https://doi.org/10.1016/j.ijpharm.2016.04.021.
34. Cao, L.; Man, T.; Kruk, M. Synthesis of Ultra-Large-Pore SBA-15 Silica with Two-Dimensional Hexagonal Structure Using Triisopropylbenzene As Micelle Expander. *Chem. Mater.* **2009**, *21*, 1144-1153, https://doi.org/10.1021/cm8012733.
35. Weng, J.; Henry, H.; Tong, Y.; Fung Chow, Y. In Vitro Release Study of the Polymeric Drug Nanoparticles: Development and Validation of a Novel Method. *Pharmaceutics* **2020**, *12*, https://doi.org/10.3390/pharmaceutics12080732.
36. Narashimhan, B.; Mallapragada, S.; Peppas, N. *Release kinetics, data interpretation, Encyclopedia of controlled drug delivery*. Mathiowitz, E. Ed., John Wiley and Sons, Inc, New York, **1999**.
37. Gibaldi, M.; Perrier, D. *Pharmacokinetics, Drugs and the Pharmaceutical Sciences*. 2nd Edition Marcel Dekker, Inc, New York and Basel, Volume 15, **1982**; https://doi.org/10.1002/bdd.2510040213.
38. Higuchi, T. Rate of release of medicaments from ointment bases containing drugs in suspension. *J. Pharm. Sci.* **1961**, *50*, 874–875, https://doi.org/10.1002/jps.2600501018.
39. Higuchi, T. Mechanism of sustained-action medication Theoretical analysis of rate of release of solid drugs dispersed in solid matrices. *J. Pharm. Sci*. **1963**, *52*, 1145–1149, https://doi.org/10.1002/jps.2600521210.
40. Higuchi, T. Mechanism of sustained action mediation: Rate of release of medicaments from ointment bases containing drugs in suspension. *J. Pharm. Sci*. **1961**, *50*, 874-5, https://doi.org/10.1002/jps.2600501018.
41. Grassi, M.; Grassi, G. Mathematical modelling and controlled drug delivery: matrix systems. *Curr. Drug Deliv*. **2005**, *2*, 97-116, https://doi.org/10.2174/1567201052772906.
42. Schott, H. Kinetics of Swelling of Polymers and Their Gels. *J. Pharm Sci.* **1992**, *81*, 467-470, https://doi.org/10.1002/jps.2600810516.
43. Weibull, W. A statistical distribution function of wide applicability. *J. Appl. Mech*. **1951**, *18*, 293–297.
44. Maxime, I.; Mykyta, V.; Chubynsky, G.; Slater, W. Interpreting the Weibull fitting parameters for diffusion-controlled release data. *Physica A* **2017**, *486*, 486–496, https://doi.org/10.1016/j.physa.2017.05.033.
45. Langenbucher, F. Linearization of dissolution rate curves by the Weibull distribution. *J. Pharm. Pharmacol.* **1972**, *24*, 979–981, https://doi.org/10.1111/j.2042-7158.1972.tb08930.x.
46. Costa, P.; Sousa, L.J. Modeling and comparison of dissolution profiles. *Eur. J. Pharm. Sci.* **2001**, *13*, 123–133, https://doi.org/10.1016/S0928-0987(01)00095-1.
47. Vudathala, G.; Rogers, J. Dissolution of fludrocortisone from phospholipid coprecipitates. *J. Pharm. Sci.* **1992**, *82*, 282–286, https://doi.org/10.1002/jps.2600810318.
48. Korsmeyer, W.; Gurny, R.; Doelker, E.; Buri, P.; Peppas, N. Mechanisms of solute release from porous hydrophilic polymers. *Intern. J. Pharm.* **1983**, *15*, 25-35, https://doi.org/10.1016/0378-5173(83)90064-9.
49. Ritger, P.; Peppas, N. A simple equation for description of solute release I. fickian and non-fickian release from non-swellable devices in the form of slabs, spheres, cylinders or discs. *J. Control. Release* **1987**, *5*, 23-36, https://doi.org/10.1016/0168-3659(87)90034-4.
50. Ritger, P.; Peppas, N. A simple equation for description of solute release II. fickian and anomalous release from swellable devices. *J. Control. Release* **1987**, *5*, 37-42, https://doi.org/10.1016/0168-3659(87)90035-6.
51. Juárez, J.; Gómez Costa, M. and Anunziata, O. Synthesis and characterization of Pt-CMK-3 hybrid nanocomposite for hydrogen storage. *Int. J. Energy Res.* **2015**, *39*, 128–139, https://doi.org/10.1002/er.3229.

52. Rokhade, A.; Agnihotri, S.; Patil, S.; Mallikarjuna, N.; Kulkarni, P.; Aminabhavi T.M. Semiinterpenetrating polymer network microspheres of gelatin and sodium carboxymethyl cellulose for controlled release of ketorolac tromethamine. *Carbohydr. Polym.* **2006**, *65*, 243–252, https://doi.org/10.1016/j.carbpol.2006.01.013.
53. Anunziata, O.A.; Martínez, M.L.; Gomez Costa, M.B. Characterization and acidic properties of Al-SBA-3 mesoporous material. *Mater. Lett.* **2010**, *64*, 545–548, https://doi.org/10.1016/j.matlet.2009.11.072.
54. López Goerne, T.M.; López Garcia, M.G.; Rodríguez Grada, G.; Ortiz Pérez, I.; Gómez López, E.; Alvarez Lemus, M.A. Obtaining of Sol-Gel Ketorolac-Silica Nanoparticles: Characterization and Drug Release Kinetics. *J. Nanomater.* **2013**, *2013*, 1-9, https://doi.org/10.1155/2013/450483.
55. Ragab, M.A.A.; El Yazbi, F.A.; Hassan, E.M.; Khamis, E.F.; Hamdy, M.M.A. Spectrophotometric analysis of two eye preparations, vial and drops, containing ketorolac tromethamine and phenylephrine hydrochloride binary mixture and their ternary mixture with chlorphenirmaine maleate. *Bull. of Fac. of Pharmacy* **2018,** *56*, 91-100, https://doi.org/10.1016/j.bfopcu.2018.03.004.
56. Amul, B.; Muthu, M.; Raja S.; Sevvanthi, S. Molecular structure, spectroscopic (FT-IR, FT-Raman, NMR, UV-VIS), chemical reactivity and biological examinations of Ketorolac. *J Mol. Struc.* **2020**, *1210*, https://doi.org/10.1016/j.molstruc.2020.128040.
57. Lin, S.; Yang, J. In vitro dissolution behaviour of some sustained-release theophylline dosage forms. *Pharm. Acta Helv.* **1989**, *64*, 236–240.
58. Sangalli, M.; Giunchedi, P.; Maggi, L.; Conte, U.; Gazzaniga, A. Inert monolithic device with a central hole for constant drug release. *Eur. J. Pharm. Biopharm.* **1994**, *40*, 370–373.
59. Abasian, P.; Ghanavati, S.; Rahebi, S.; Nouri Khorasani, S.; Khalili, S. Polymeric nanocarriers in targeted drug delivery systems: A review. *Polym. Adv. Technol.* **2020**, *31*, 2939–2954, https://doi.org/10.1002/pat.5031.
60. Pedersen, P.; Myrick, J. Versatile kinetic approach to analysis of dissolution data. *J. Pharm. Sci.* **1978**, *67*, 1450–1455, https://doi.org/10.1002/jps.2600671034.
61. Christensen, F.; Hansen, F.; Bechgaard, H. Physical interpretation of parameters in the Rosin–Rammler–Sperling–Weibull distribution for drug release from controlled release dosage forms. *J. Pharm. Pharmacol.* **1980**, *32*, 580–582, https://doi.org/10.1111/j.2042-7158.1980.tb13002.x.
62. Corsaro, C.; Neri, G.; Mezzasalma, A.M.; Fazio, E. Weibull Modeling of Controlled Drug Release from Ag-PMA Nanosystems. *Polymers* **2021**, *13*, https://doi.org/10.3390/polym13172897.
63. Agnihotri, S.; Aminabhavi, T. Controlled release of clozapine through chitosan microparticles prepared by a novel method. *J. Control. Release* **2004**, *96*, 245-259, https://doi.org/10.1016/j.jconrel.2004.01.025.
64. Gupta, J.; Gupta, R.; Vanshita. Microneedle Technology: An Insight into Recent Advancements and Future Trends in Drug and Vaccine Delivery. *Assay Drug Dev Technol.* **2021**, *19*, 97-114, https://doi.org/10.1089/adt.2020.1022.
65. Wang, J.; Wu, W.; Lin, Z. Kinetics and thermodynamics of the water sorption of 2-hydroxyethyl methacrylate/styrene copolymer hydrogels. *J. Appl. Polym. Sci.* **2008**, *109*, 3018–3023, https://doi.org/10.1002/app.28403.
66. Juárez, J.; Cussa, J.; Gómez Costa, M.; Anunziata, O. Nanostructured Ketorolac-Tromethamine/MCF: Synthesis, Characterization and Application in Drug Release System. *Curr. Nanosci.* **2018**, *14*, 1-8, https://doi.org/10.2174/1573413714666180222134742.
67. Rokhade, A.; Agnihotri, S.; Patil, S.; Mallikarjuna, N.; Kulkarni, P.; Aminabhavi, T. Semi-interpenetrating polymer network microspheres of gelatin and sodium carboxymethyl cellulose for controlled release of ketorolac tromethamine. *Carbohydr. Polym.* **2006**, *65*, 243-252, https://doi.org/10.1016/j.carbpol.2006.01.013.
68. Saurí, J.; Millán D.; Suñé-Negre, J.; Colom, H.; Ticó, J.; Miñarro, M.; Pérez-Lozano, P.; García-Montoya, E. Quality by Design approach to understand the physicochemical phenomena involved in controlled release of captopril SR matrix tablets. *Int. J. Phar.* **2014**, *477*, 431–441, https://doi.org/10.1016/j.ijpharm.2014.10.050.
69. Mitchell, M.J.; Billingsley, M.M.; Haley, R.M.; Wechsler, M.E.; Peppas, N.A.; Langer, R. Engineering precision nanoparticles for drug delivery. *Nature Reviews Drug Discovery* **2021**, *20*, 101-124, https://doi.org/10.1038/s41573-020-0090-8.
70. Muhammad, P.; Hanif, S.; Yan, J.; Rehman F.; Wang, J.; Khan, M.; Chung, R.; Lee, A.; Zheng, M , Wang, Y.; Shi, B. SERS-based nanostrategy for rapid anemia diagnosis. *Nanoscale* **2020**, *12*, 1948-1957, https://doi.org/10.1039/c9nr09152a.
71. Anunziata, O.; Gómez Costa, M.; Martínez, M. Interaction of water and aniline adsorbed onto Na-AlMCM-41 and Na-AlSBA-15 catalysts as hosts materials. *Catal. Today* **2008**, *133-135*, 897-905, https://doi.org/10.1016/j.cattod.2007.12.073.